International Journal of Power Electronics and Drive System (IJPEDS)
Vol. 8, No. 2, June 2017, pp. 623~638
ISSN: 2088-8694, DOI: 10.11591/ijpeds.v8i2.pp623-638

Dynamic Modeling and Simulation of Short-Duration Over-excitation Phenomenon in Hysteresis Motor

Sayyed Hossein Edjtahed[1], Amir Hossein Pir Zadeh[2], Abolfazl Halvaei Niasar[3]
Department of Electrical and Computer Engineering, University of Kashan, Kashan, Iran

Article Info

Article history:

Received Jan 3, 2017
Revised Mar 3, 2017
Accepted Mar 17, 2017

Keyword:

B-H loop
Dynamic modeling
Electrical motor
Hysteresis motor
Over-excitation
Simulation

ABSTRACT

The hysteresis motor is a well-known synchronous motor that is used in special small power, high speed applications. Dynamic modeling and analysis of this motor is more complicated than permanent magnet synchronous motors (PMSMs) or induction motors (IMs) due to nonlinear behavior of rotor magnetic material. Short over-excitation is a unique phenomenon that only occurs in hysteresis motor in which the terminal voltage increase at synchronous speed for a short duration, and then continuously is decrease to initial value. Therefore, the input current is reduced, this leads to more power factor and efficiency enhancement. Till now, there isn't any analytic dynamic model of this phenomenon. In this paper, based on a novel dynamic model of hysteresis motor, the over-excitation phenomenon is investigated and transient performance of the motor during over-excitation is simulated via Simulink.

Corresponding Author:

Abolfazl Halvaei Niasar,
Department of Electrical and Computer Engineering,
University of Kashan,
Tel/Fax: +98-31-55912412, P.O.Box 87317-51167, Kashan, Iran,
E-mail: halvaei@kashanu.ac.ir

1. INTRODUCTION

The hysteresis motor can be regarded as a self-starting synchronous machine, which has the same structure as squirrel cage asynchronous motor with exception that its rotor consist of a ring of magnetic material which covers a non-magnetic core. It is often used for small power application that needs a very smooth torque at high speed such as gas centrifuge and gyroscope [1]. Relatively low starting current, simple and strong structure, uniform torque-speed characteristic and also low power factor, low efficiency and hunting phenomenon are some of hysteresis motor advantages and disadvantages [2]. There are two main structures for hysteresis motors; cylindrical and disk types as shown in Figure 1. Cylindrical hysteresis motors are classified in two types of circumferential-flux and radial-flux. In circumferential-flux hysteresis motor, the rotor ring is mounted on non-magnetic material as support. The magnetic field lines in the rotor are mostly circumferential to the ring. This type of hysteresis motor is mostly used in industrial applications [3].

Since the power factor of hysteresis motor is much lower than that of an induction motor, it takes more RMS current and hence large capacity condensers are installed to enhance the power factor. However, this is not favorable because resonance is caused by the presence of hysteresis motor inductance and condenser capacitance and efficiency is not improved. Rotors showed that the over-excitation for a short period of the hysteresis motor running at synchronous speed causes the reduction of the stator current and the increase of the pullout torque at the same time [4]. This phenomenon is very important from the view point of high-efficiency operation and has been discussed by some researchers [5]-[8]. They have investigated the over-excitation, but couldn't model this phenomenon. Lately, over-excitation has been experienced via variable frequency inverters and various voltage patterns have been applied to hysteresis motor to gain more

efficient performance for hysteresis motor [9]-[11]. But it has not presented any dynamic model to predict the transient performance of hysteresis motor during over-excitation. This paper investigates the transient behavior of the motor during short over-excitation based on a novel dynamic model for hysteresis motor. The paper is organized as follows: In section 2, the over-excitation phenomenon is described briefly. Section 3 proposes a novel dynamic model of hysteresis motor. In section 4, some simulation results are given and then conclusion is explored in section 5.

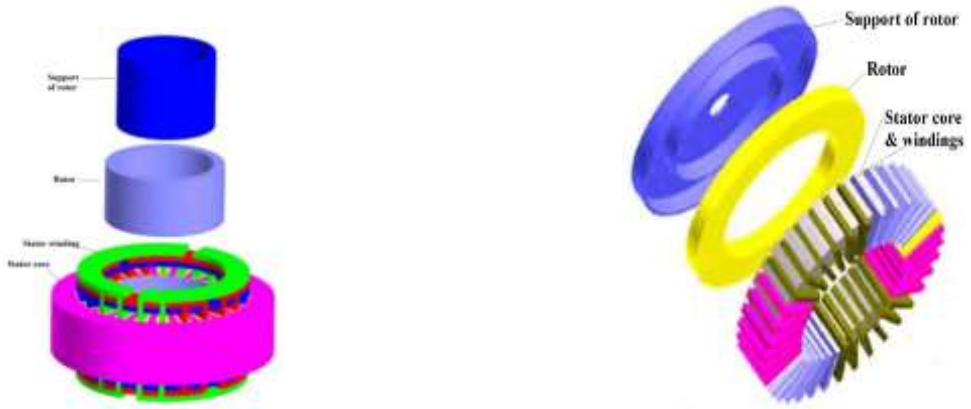

(a) (b)

Figure 1. Structure of various types of hysteresis motor: (a) Circumferential-flux (b) Axial-flux

2. SHORT-DURATION OVER-EXCITATION PHENOMENON

Short-duration or short Over-excitation is an effective process for increasing output power, improving power factor and efficiency and reducing input current [12]. Over-excitation means that the input voltage V_i applied to a motor operating at synchronous speed is increased continuously up to nV_i ($n > 1$) and then continuously decreased up to V_i. Factor n is called over-excitation factor.

2.1. Terminal Voltage Pattern with Short-Duration Over-excitation

Figure 2 shows the method for the over-excitation considered here. The motor is accelerated to its synchronous speed at a stator voltage V_i. After synchronization, the stator voltage is raised to a higher value nV_i for a short period, and then reduced to the original value V_i. It is assumed that the load torque remains constant during this change. In this paper a circumferential-flux type hysteresis motor is analyzed, although the following method can also be extended to radial-flux type hysteresis motor.

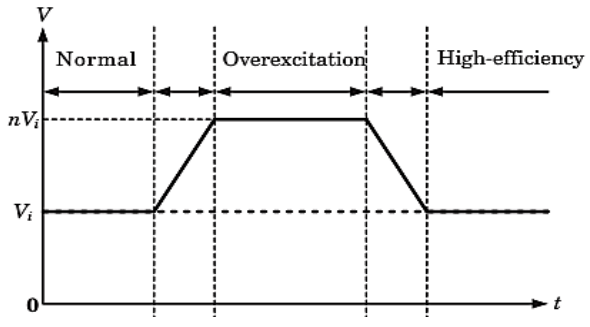

Figure 2. Terminal voltage pattern [11]

2.2. Magnetic Behavior of Rotor Hysteresis Material before and after Over-excitation

Let us first investigate the magnetic state of rotor before over-excitation. When the rotor turns at sub-synchronous speed, any point in rotor hysteresis material experiences a sinusoidal variation of flux

density B in time, and consequently a magnetic hysteresis loop L_0 shown in Figure 3(a). Other points in the rotor hysteresis material experience exactly the same hysteresis loop, displaced in time phase. Thus the loop not only gives the time variation of magnetic state at a point in the rotor, but also gives space variation of magnetic state around rotor at a particular instant of time [7,13]. The area of this loop is proportional to output torque T_{em}. When the motor reaches to synchronous speed, magnetic state at any point momentarily stops changing. For example, the magnetic state at a point P in Figure 3(b) in the rotor stops at the location of P_0 on the loop shown in Figure 3(a), and the magnetic state at another point stops at Q_0 on the same loop. If the load torque is equal to output torque T_{em}, motor speed will not change further. But, if the load torque is less than T_{em}, the motor speed will increase further and a displacement of the rotor forward with respect to the rotating flux density wave will occur. So, points of P_0-Q_0 come to P_1-Q_1 that means the operational B-H loop goes to other loop L_1. Hence, a new B-H loop is created that its area is smaller than loop L_0. It means that with changing load torque, the B-H loop will not be fixed. The same behavior can be explained when the load torque increases, so that loop L_1 will be wider than loop L_0. The shape of L_1 is different from the major hysteresis loop created by rated input voltage or from those of the minor hysteresis loops created by lower voltages. Since the area of the B-H loop is proportional to the output torque [1], the area of loop L_1 is proportional to output torque witch is in equilibrium with load torque.

Now, let us investigate the change in the magnetic state of the rotor when it is overexcited. When the stator voltage is increased from V_i to nV_i, the flux density in the rotor also increases. Therefore, the points P_1, Q_1 on loop L_1 will ascend along their respective minor loops toward the ascending branch of the major loop L_0 in Figure 4(a). The points that meet the ascending branch of loop L_0 will go up further along it the points that pass the tip of the major loop L_0 will ascend along the normal magnetization curve of the rotor hysteresis material. For example, the points P_1-Q_1 will come to P_2-Q_2, respectively. Thus, the B-H relation around the rotor is given by a closed loop L_2 in Figure 4(a). It should be noted that load torque remains unchanged during mentioned process. This means that the area of loop L_2 must be equal to that of loop L_1. In other words, amplitude and phase of flux density distribution in the rotor are such that the areas of both loops are equal. Such flux density distribution and therefore loop L_2, can be obtained from an iterative calculation. When stator voltage is reduced from nV_i to original value V_i, the flux density in rotor now decreases. Therefore, for example, points P_2 and Q_2 on loop L_2 descend along the descending branch of the respective major loops whose tips are P_2 and Q_2, and come to P_3 and Q_3, respectively, as shown in Figure 4(a). Thus, the B-H relation around the rotor is given by a closed loop L_3. The area of loop L_3 must be equal to that of loop L_2, because the load torque is constant. If the load torque is increased, there will be a decrease of speed and a displacement of the rotor backward with respect to rotating flux. Then, for example, the flux density at point P decreases to P_4 and the flux density at point Q increase to Q_4 as shown in Figure 4(b). As a result, the B-H relation given by loop L_4 in Figure 4(a) can be obtained, the area of which is corresponding to the pull-out torque after over-excitation [7].

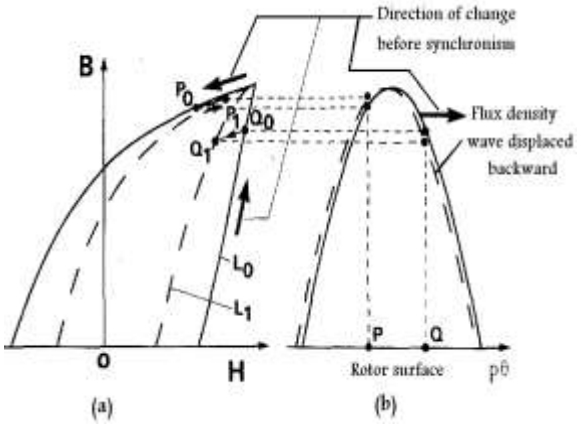

Figure 3. B-H loops and flux density waves for two different loads [7,13], (L1 loop corresponds to the lower load)

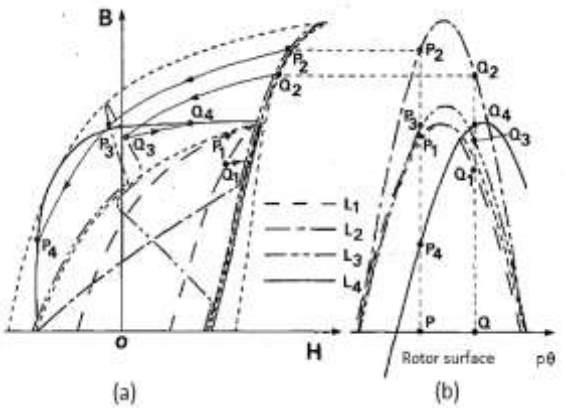

Figure 4. B-H loops and flux density waves during over-excitation process [7]

3. DYNAMIC MODEL of HYSTERESIS MOTOR

The common point in all mentioned steady-state equivalent circuit models is that the rotor's hysteresis loop is considered as hysteresis resistance R_h in series with reactance X_h in sub synchronous mode as shown in Figure 5. In this section a new dynamic model for hysteresis motor with incorporating the change of load torque and stator voltage to identify the operational B-H loop of rotor is developed [14].

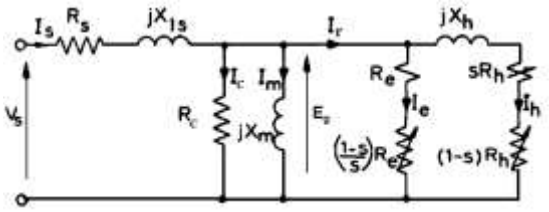

Figure 5. Equivalent circuit of hysteresis motor at sub synchronous mode [15]

3.1. Calculation of Rotor's Equivalent Circuit Parameters

Hysteresis motor used in this paper is a super-high speed circumferential-flux type motor, 3-phases, star-connected, with given parameters in Table 1. To develop dynamic model of hysteresis motor, the value of rotor's parameters due to operational hysteresis motor must be calculated. For this purpose B-H curves of rotor material are firstly measured by some standard experiments [16]. Employed magnetic material used in this study is Vicalloy 2 with typical B-H loops shown in Figure 6. Maximum achieved output hysteresis torque in steady state is corresponding to maximum applied voltage to stator that is proportional to major hysteresis loop. For simplicity of calculation, the fundamental harmonic of magnetic field intensity (*H*) and field density (*B*) are just considered that means the hysteresis loops are considered as elliptical.

Table 1. Rated specifications and parameters of used circumferential-flux hysteresis motor

Symbol	Quantity	Value	Dimension
V_{rated}	line rated voltage	230	V
T_{rated}	rated torque	0.01	N.m
f_{rated}	rated frequency	1000	Hz
ω	supply angular frequency	$2\pi\times1000$	rad/sec
m	number of phase	3	
P	number of poles	2	
J	shaft inertia moment	3×10^{-9}	$kg.m^2$
R_s	stator resistance	16.4	Ω/ph
R_c	stator core loss equivalent resistance	10580	Ω/ph
R_h	rated rotor hysteresis resistance	300	Ω/ph
R_e	eddy current resistance of rotor	223	Ω/ph
X_{ls}	stator leakage reactance	78	Ω/ph
X_m	rated magnetizing reactance	400	Ω/ph
X_h	rated rotor hysteresis reactance	170	Ω/ph
l_h	axial length of hysteresis ring	25	mm
g	air gap length	1	mm
r_q	mean radius of air gap	24.45	mm
β	hysteresis lag angle	60^o	
ρ	electrical resistivity of hysteresis ring	650	μΩ·mm
μ_r	relative permeability of hysteresis ring	20	
μ_0	permeability of free space	$4\pi\times10^{-7}$	H/m

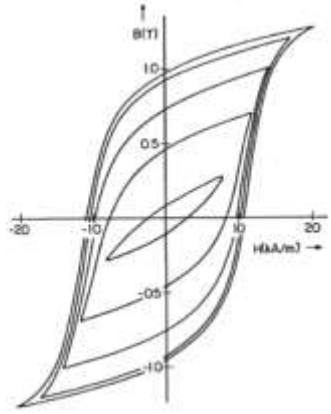

Figure 6. B-H characteristics for a typical Vicalloy magnetic material used in hysteresis motor [17]

The flowchart for calculation of the motor's parameters in air gap and rotor circuit is shown in Figure 7. Firstly, the operational B-H loop or corresponding lag angle β due to applied stator voltage V_{in} is identified and then is modified based on applied load torque using equivalent circuit shown in Figure 5. In this circuit, $R_s + jX_{ls}$ is stator leakage impedance, $R_c \parallel jX_m$ is air gap impedance, and $(R_h + jX_h) \parallel R_e / s$ is equivalent rotor impedance. The air gap reactance and rotor impedance are expressed as [18]:

$$X_m = \frac{2m\omega\left(K_w N_{ph}\right)^2 \mu_0 r_g l_h}{\pi P^2 g} \tag{1}$$

$$R_h = \frac{m\omega\left(K_w N_{ph}\right)^2 \mu V_r}{\pi^2 r_h^2} \sin\beta \tag{2}$$

$$X_h = \frac{m\omega\left(K_w N_{ph}\right)^2 \mu V_r}{\pi^2 r_h^2} \cos\beta \tag{3}$$

To calculate the eddy current resistance in hysteresis material of the rotor, it should be noted the flux flow in rotor is circumferential and the eddy current vector is perpendicular to the flux. So, eddy current resistance can be obtained from:

$$R_e = \frac{2\rho l_h}{A_h} \tag{4}$$

The hysteresis ring volume V_r and cross sectional area A_h in (2)-(4) are calculated from:

$$A_h = 2\pi r_h t_r \tag{5}$$

$$V_r = A_h l_h = 2\pi r_h t_r l_h \tag{6}$$

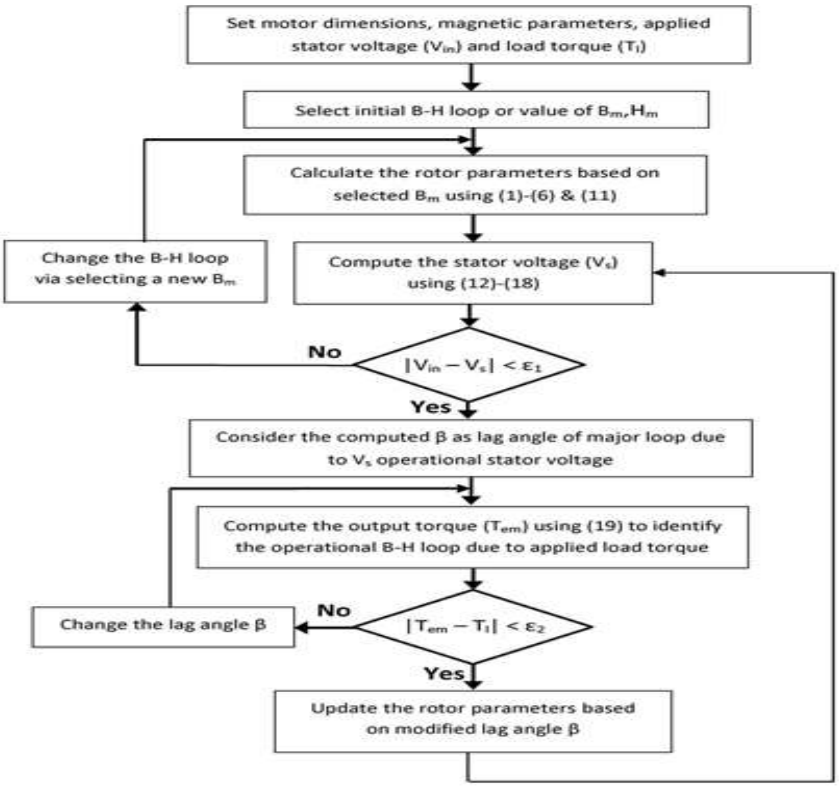

Figure 7. Flowchart for calculation of the rotor's equivalent circuit parameters [18]

To identify the hysteresis lag angle β due to operational stator voltage V_{in}, firstly an initial B-H curve (or initial H_m and B_m) is chosen. Suppose the fundamental harmonic of magnetic field intensity in the rotor is defined as:

$$H = H_m \cos \omega t = \left(B_m / \mu \right) \cos \omega t \tag{7}$$

So, flux density in rotor can be expressed as:

$$B = a \cos \omega t + b \sin \omega t = B_m \cos(\omega t - \beta) \tag{8}$$

Corresponding to measured B-H loops, parameters of a, b can be calculated for any given H_m and created B_m. For an elliptical B-H loop with area of W_h, the parameter of b is related to W_h through:

$$b = \frac{W_h}{\pi H_m} \tag{9}$$

and coefficient 'a' is derived from:

$$a = \sqrt{B_m^2 - b^2} \tag{10}$$

Therefore, the hysteresis lag angle β is obtained by:

$$\beta = \tan^{-1}(b/a) \tag{11}$$

which it varies from 40° to 70° for semi-hard magnetic material used in this study. Now as shown in Figure 8, for obtained lag angle β, the equivalent circuit's parameters are calculated. To check the validity of β, computed input voltage of stator is compared with real stator voltage. To compute the stator voltage V_s, induced voltage in air gap is calculated from:

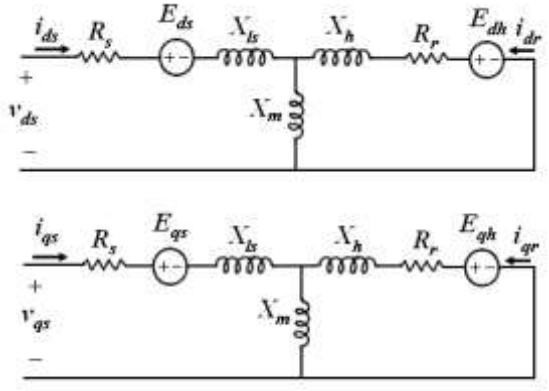

Figure 8. Equivalent circuit for dynamic model of hysteresis motor in rotating dq reference frame

where ϕ_g represents the air gap flux per pole, and is obtained for a cylindrical machine with selected value of B_m by:

$$\phi_g = 2K_{sf}\, l_h r_g B_m \tag{13}$$

The stator input current from steady-state equivalent circuit shown in Figure 5 can be obtained from:

$$\vec{I}_s = \sqrt{\left(\frac{E_g}{R_c}+\frac{E_g}{R_e/s}+\frac{E_g}{Z_h}\cos\beta\right)^2+\left(\frac{E_g}{X_m}+\frac{E_g}{Z_h}\sin\beta\right)^2}\angle-\theta_g \tag{14}$$

that the stator phase voltage is considered as reference phasor and θ_g is the phase difference between $\vec{E}_g$ and $\vec{I}_s$ as:

$$\theta_g = tan^{-1}\left(\frac{\frac{1}{X_m}+\frac{\sin\beta}{Z_h}}{\frac{1}{R_c}+\frac{1}{R_e/s}+\frac{\cos\beta}{Z_h}}\right) \tag{15}$$

and the impedance due to hysteresis material is:

$$Z_h = \sqrt{R_h{}^2 + X_h{}^2} \tag{16}$$

Therefore, the input voltage is calculated by:

$$V_{in} = \sqrt{\left(E_g\cos\theta_g + Z_s I_s\cos\theta_s\right)^2+\left(E_g\sin\theta_g + Z_s I_s\sin\theta_s\right)^2} \tag{17}$$

where Z_s, θ_s are the stator's impedance and argument as:

$$Z_s = \sqrt{R_s{}^2 + X_{ls}{}^2}\ ,\ \theta_s = tan^{-1}\left(X_{ls}/R_s\right) \tag{18}$$

The error between calculated input voltage V_{in} by (17) and real stator voltage should be less than $\varepsilon_1 = 0.01\,V$. Otherwise the chosen B-H curve is changed by modifying of H_m by a proper step size, and the calculations are repeated until the error falls into ε_1 tolerance. As mentioned earlier, when the hysteresis motor reaches synchronous speed, developed torque T_{em} is equal to load torque T_l. The steady-state developed torque in terms of hysteresis ring's volume, operational B-H loop properties and lag angle β can be expressed as [19]:

$$T_{em} = \frac{mP}{2}\pi(B_m H_c) r_h t_r l_h \sin\beta \tag{19}$$

It means that if under constant stator voltage, the load torque varies, operational B-H loop changes without changing value of B_m and H_m and so the lag angle β varies as shown in Figure 3. Therefore, in final stage of computation, developed torque T_{em} through (6) is compared with the load torque and lag angle β is iterated by a proper step size until the torque difference falls to desired tolerance $\varepsilon_2 = 0.0005\ N.m$ as shown in Figure 7. The computed lag angle β is then used to update the rotor's equivalent circuit parameters.

Hysteresis motors use the semi-hard magnetic materials that unlike to induction motors induce considerable back-EMF voltage in stator. For dynamic modeling of hysteresis motor, it is necessary to consider an induced voltage source in rotor circuit. This equivalent induced voltage E_h for hysteresis material can be obtained from Figure 5 as:

$$\vec{E}_h = \sqrt{\left(X_m I_s \sin\theta_g + \left(X_h + X_m\right) I_h \sin\beta\right)^2 + \left(X_m I_s \cos\theta_g + \left(X_h + X_m\right) I_h \cos\beta\right)^2}\ \angle\theta_h \tag{20}$$

Where

$$\theta_h = tan^{-1}\left(\frac{X_m I_s \cos\theta_g + \left(X_h + X_m\right) I_h \cos\beta}{X_m I_s \sin\theta_g + \left(X_h + X_m\right) I_h \sin\beta}\right) \tag{21}$$

Calculated E_h is a phasor corresponding to phase 'a'. It has to be expressed in time domain for three phases and then transferred to E_{dh} and E_{qh} in dq reference frame. These voltages at synchronous condition are constant.

3.2. Mathematical Model and Equivalent Circuit of Hysteresis Motor in Rotating dq Reference Frame

The hysteresis motor voltage equations in synchronously rotating dq reference frame can be written as:

$$V_{dq} = R \cdot I_{dq} + \frac{d\Lambda_{dq}}{dt} + E_{dq} \tag{22}$$

where,

$$V_{dq} = \begin{bmatrix} v_{ds} \\ v_{qs} \\ v_{dr} = 0 \\ v_{qr} = 0 \end{bmatrix},\ I_{dq} = \begin{bmatrix} i_{ds} \\ i_{qs} \\ i_{dr} \\ i_{qr} \end{bmatrix},\ \Lambda_{dq} = \begin{bmatrix} \lambda_{ds} \\ \lambda_{qs} \\ \lambda_{dr} \\ \lambda_{qr} \end{bmatrix},\ E_{dq} = \begin{bmatrix} E_{ds} \\ E_{qs} \\ E_{dh} \\ E_{qh} \end{bmatrix} \tag{23}$$

and,

$$R=\begin{bmatrix} R_s & 0 & 0 & 0 \\ 0 & R_s & 0 & 0 \\ 0 & 0 & R_r & 0 \\ 0 & 0 & 0 & R_r \end{bmatrix} \tag{24}$$

where the rotor resistance is calculated from:

$$R_r=\frac{1}{1/R_h+s/R_e} \tag{25}$$

and '*s*' denotes the slip. The stator and rotor fluxes in (22) are:

$$\Lambda_{dq}=L\times I_{dq}=\begin{bmatrix} L_s & 0 & 0 & 0 \\ 0 & L_s & 0 & 0 \\ 0 & 0 & L_r & 0 \\ 0 & 0 & 0 & L_r \end{bmatrix}\times\begin{bmatrix} i_{ds} \\ i_{qs} \\ i_{dr} \\ i_{qr} \end{bmatrix} \tag{26}$$

where the inductances are calculated from:

$$L_s=L_{ls}+L_m,\ \ L_r=L_h+L_m \tag{27}$$

The magnetizing and rotor inductances L_m, L_h can be calculated from (1) and (3). Two voltages E_{ds}, E_{qs} in (23) are defined by:

$$E_{ds}=-\omega_r\lambda_{qs},\qquad E_{qs}=\omega_r\lambda_{ds} \tag{28}$$

Also E_{dh} and E_{qh} are dq components of induced voltage due to residual magnetizing action of hysteresis material on the rotor that are obtained using (20) as follows:

$$\begin{bmatrix} E_{dh} \\ E_{qh} \end{bmatrix}=\left[T_{dq}(\theta_r)\right]\begin{bmatrix} E_h\sin\omega t \\ E_h\sin(\omega t-120^o) \\ E_h\sin(\omega t+120^o) \end{bmatrix} \tag{29}$$

That the following Park matrix is used for abc to dq transformation [20]-[22]:

$$\left[T_{dq}(\theta_r)\right]=\frac{2}{3}\begin{bmatrix} \cos\theta_r & \cos(\theta_r-120^o) & \cos(\theta_r+120^o) \\ \sin\theta_r & \sin(\theta_r-120^o) & \sin(\theta_r+120^o) \\ \frac{1}{2} & \frac{1}{2} & \frac{1}{2} \end{bmatrix} \tag{30}$$

Developed electromagnetic torque can be expressed in term of flux and current as:

$$T_{em}=\frac{3}{2}\frac{P}{2}(\lambda_{ds}i_{qs}-\lambda_{qs}i_{ds}) \tag{31}$$

and the mechanical speed is obtained from:

$$J\frac{d\omega_r(t)}{dt}=T_{em}-T_l \tag{32}$$

The foregoing equations can be summarized in the equivalent circuit model as shown in Figure 8.

4. SIMULATION RESULTS

Some simulations are explored for a hysteresis motor with parameters summarized in Table 1. It should be noted that employed hysteresis motor in this study is a super high-speed motor with rated speed 60,000 rpm in which its start-up procedure from zero to final speed takes 4200 sec with a slow acceleration rate. Simulation of this duration takes very much computation and needs a lot of RAM and memory. Therefore, to shorten the simulation time to 2 seconds, we are forced to decrease the inertia moment adequately. Before simulation of over-excitation phenomenon, developed dynamic model is simulated to confirm the theoretical aspects of hysteresis motor. To have better realization, some of quantities are given in per unit scale. The predominant load of employed hysteresis motor is rotational friction as $T_l = B_f \cdot \omega_m^2$ that the value of B_f is 1 in per unit scale. Although an extra constant load at synchronous speed is applied to hysteresis motor.

Figure 9 to Figure 12 show the simulation results of hysteresis motor during start-up with open-loop V/f scalar control scheme. In addition to rotational friction load, a constant load is applied. Figure 9 shows the applied reference frequency and applied stator phase voltage. In figure 10, the speed and torque response of motor are depicted during startup. The speed reaches synchronous speed under friction and constant load. The speed tracking error during start-up is at most 0.5% and becomes zero at steady-state. Moreover, when a constant load torque 0.5 pu is applied at time 1.5 sec, the motor can reach to synchronous speed after some oscillations. The RMS current, input power and power factor waveforms are shown in Figure 11. The current under rated torque 1 pu at steady-state $(t = 1.2sec)$ is 0.19 A (close to actual current of the motor in experiment). When the load torque increases to 1.5 pu, the current increases small value and reaches to 0.23 A. It is accordance to behavior of an actual hysteresis motor. The input power of the motor at steady state is 42 W includes of output power and stator's copper and core losses. With increasing the load torque, the power also increases 50%. Also the power factor firstly is 0.54 and after 1.5 sec, increases to 0.72. In Figure 12 the variations of hysteresis lag angle and rotor parameters are displayed. The angle β is increasing as well as the stator voltage increases during V/f and after 1 sec it converges to 55°. Also, at time 1.5 sec and after increasing the load torque, it converges to higher value 60°. It means that during startup or load changing, the operational B-H loop continuously changes and finds corresponding B-H loop after 1 sec when the voltage and speed become constant. Also, the values of R_h, X_h are changing with β through (8)-(9).

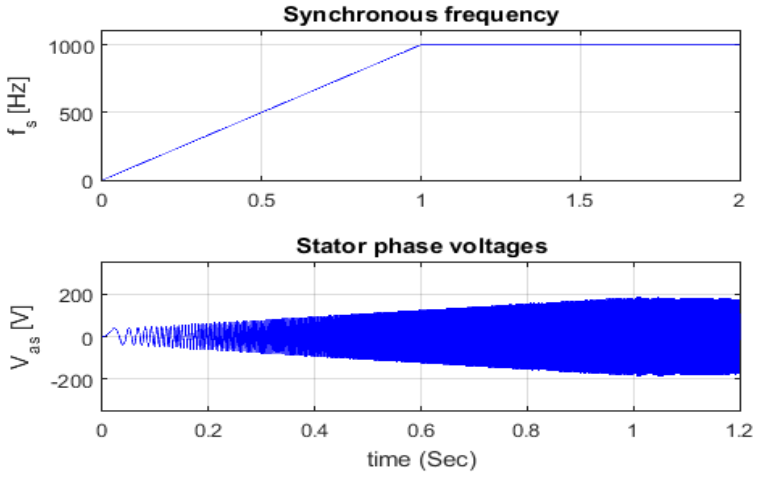

Figure 9. Reference frequency and applied phase voltage to hysteresis motor during open-loop V/f

scheme start-up

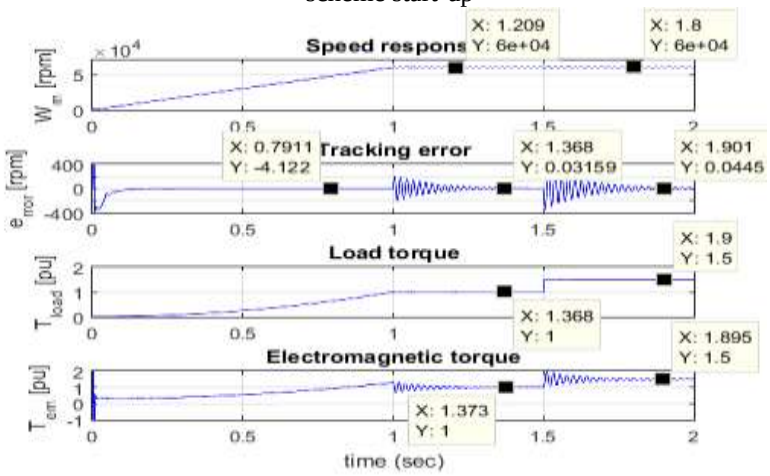

Figure 10. Speed and torque response of hysteresis motor during open-loop V/f scheme start-up

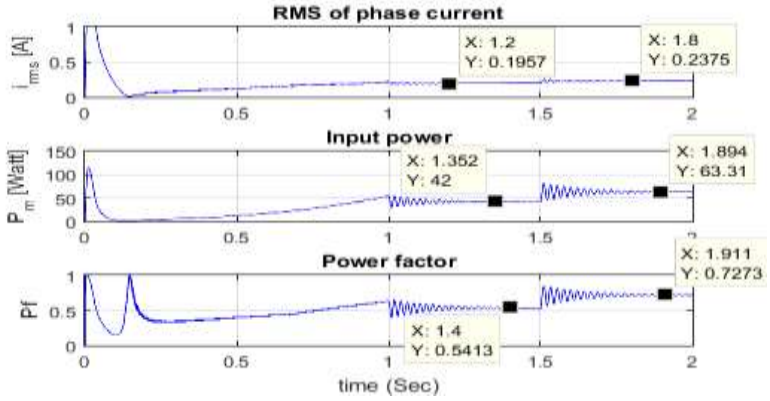

Figure 11. RMS current, input power and power factor of hysteresis motor during open-loop V/f scheme start-up

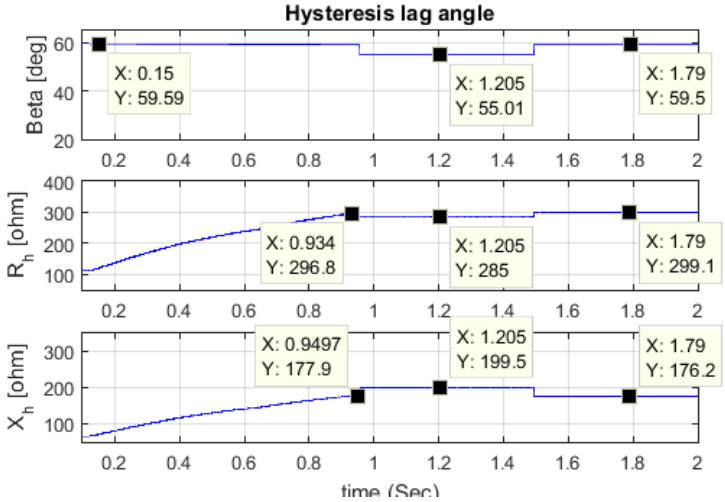

Figure 12. Variations of hysteresis lag angle β and R_h, X_h of rotor's circuit model

Now, the short-duration over-excitation is simulated based on developed dynamic model. Figure 13

shows the current and power factor of motor for over-excitation factor (n=1.25). Input current decreases after reduction input voltage from 0.19 A to 0.13 A. It means the cupper loss of stator reduces 4 times than before over-excitation. On the other hand, power factor increases from 0.54 to 0.77 that means a 50% enhancement.

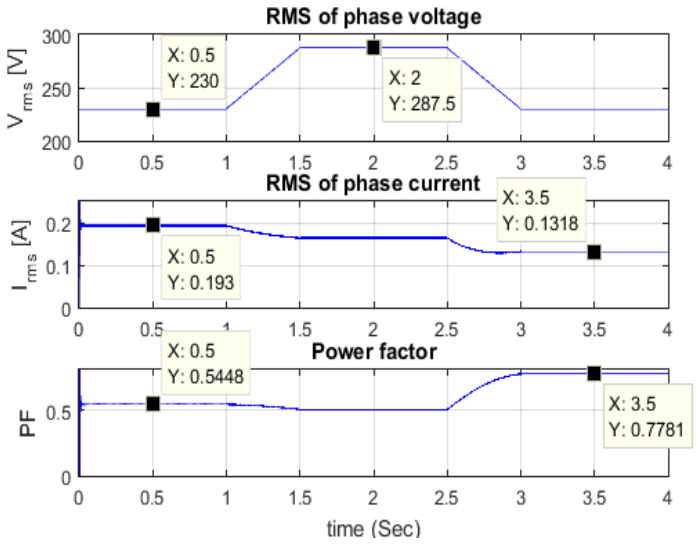

Figure 13. Input voltage, current, power factor before and after over-excitation with n=1.25

Figure 14 shows the variations of lag angle β and rotor's impedance components due to hysteresis material of rotor. During over-excitation, lag angle decreases and then it increases. The variations of R_h and X_h obey (2)-(3).

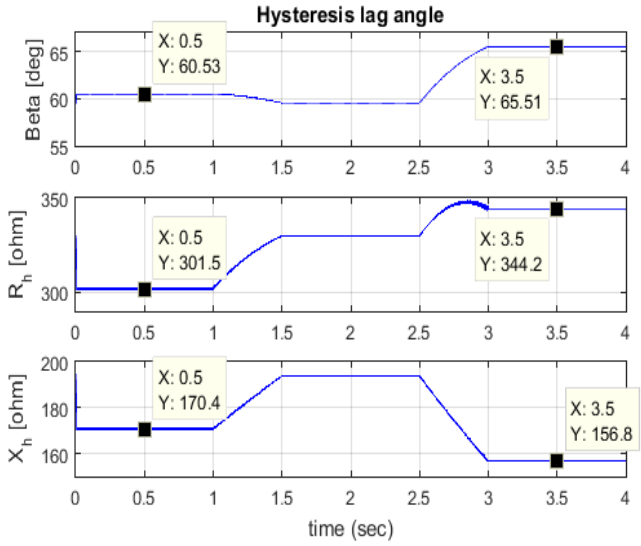

Figure 14. Lag angle β, Rh and Xh before and after over-excitation with n=1.25

Figure 15 shows the current and power factor of motor for n=1.1. The RMS value of current decreases form 0.19 A to 0.16 A, and the power factor increases from 0.54 to 0.64. Comparing of the results shown in Figure 13 and Figure 15 proves that the larger increase of terminal voltage pattern leads to better performance and higher power factor and efficiency. Using developed dynamic model of hysteresis motor, it

is possible to predict the best choice for order "n" for over-excitation process.

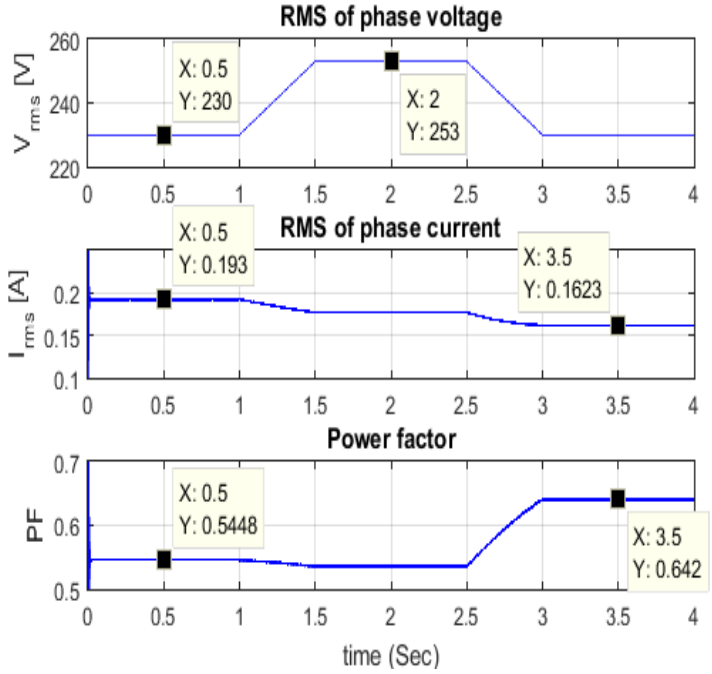

Figure 15. Input voltage, current, power factor before and after over-excitation with n=1.1

Figure 16 shows the result of over-excitation process with step change of terminal voltage and n=1.25. The enhancement of power factor and reduction in RMS current is identical to ramp variation in terminal voltage.

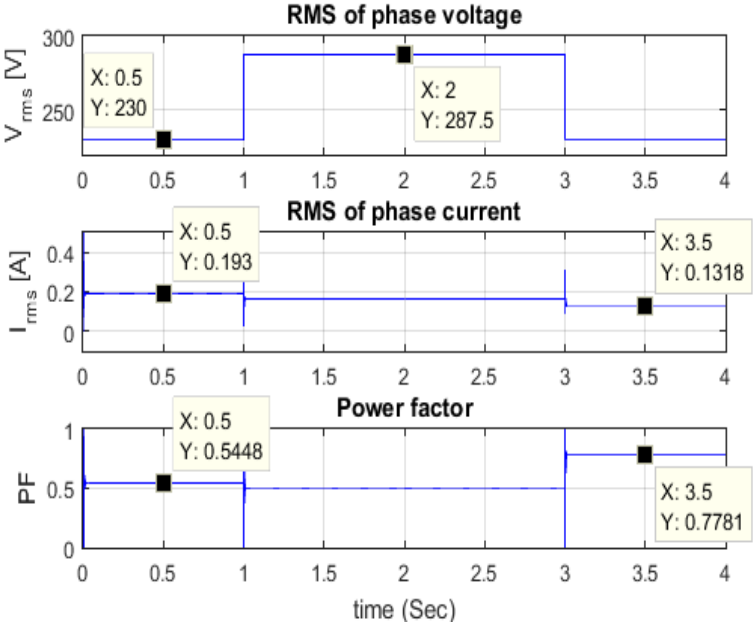

Figure 16. Input voltage, current, power factor before and after over-excitation for step change of voltage with n=1.25

However as shown in Figure 17, the fluctuation of speed for step change of the voltage is higher than ramp change.

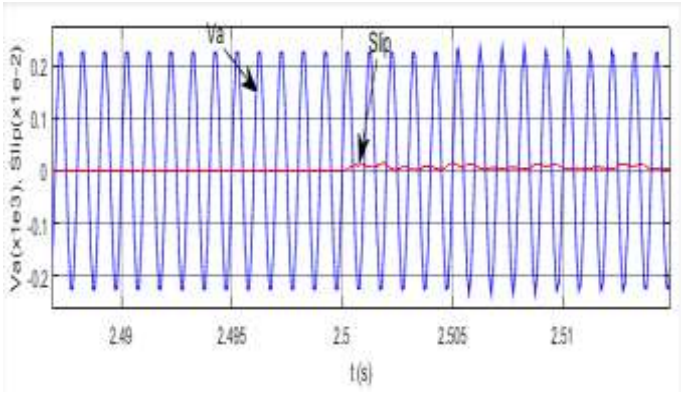

(a)

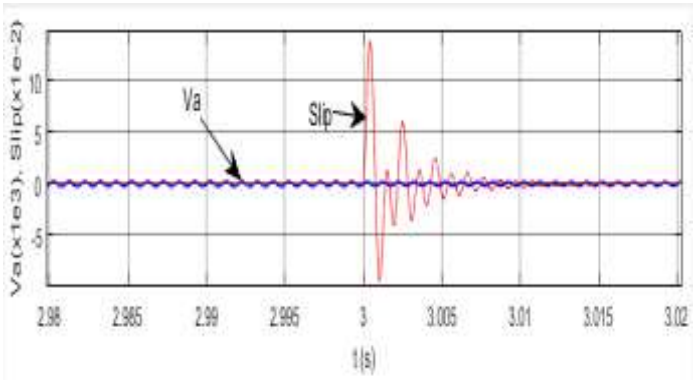

(b)

Figure 17. Changes of slip and voltage before and after over-excitation for (a) ramp change (b) step change of terminal voltage with n=1.25

5. CONCLUSION

Short duration over-excitation increases the efficiency, power factor and pull-out torque of hysteresis motor and makes it possible to operate in efficient condition. Determination of voltage amplitude and time duration in over-excitation process is essential to attain the best operational point. In this paper, the short over-excitation phenomenon of a hysteresis motor has been modeled and simulated for the first time. On this way, a novel dynamic model of hysteresis motor in rotation dq reference frame was presented. In developed model, the operational B-H curve of the motor is considered during change of input voltage or load torque. Simulation results show the effectiveness of developed model to predict the motor performance during over-excitation. The results confirm that with higher change of ststor voltage, the stator current reduces more and so the power factor increases. Moreover, step change in input voltage leasd to more hunting of speed. By using developed model it is possible to evaluate the effect of motor parameters, B-H characteristics of rotor material, magnitude of input voltage, time duration and acceleration/deceleration of voltage variations during short-over-excitation process.

REFERENCES

[1] B.R. Teare, Theory of Hysteresis Motor Torque, *AIEE Trans.*, 59, 1940, pp. 907-912.
[2] M.A. Copeland, G.R. Slemon, An Analysis of the Hysteresis Motor: part-I-Analysis of the Idealized Machine, *IEEE Trans. on Power Apparatus and System*, 82 (65), 1963, pp. 34-42.
[3] M.A. Copeland, G.R. Slemon, An Analysis of the Hysteresis Motor: part-II-The Circumferential-flux Machine, *IEEE Trans. on Power Apparatus and Systems*, 83 (6), 1964, pp. 619-625.
[4] C.H. Roters, The hysteresis motor-advances which permit economical fractional horsepower ratings, *Trans. of the American Institute of Electrical Engineers*, 66 (1), 1947, pp. 1419-1430.

[5] D. O'Kelly, Hysteresis motor with over-excitation and solid state control, *IEE Proc.*, 120, 1973, pp. 1533-1537.
[6] G. Wakui, S. Nishino, Performance of hysteresis motor after short duration over-excitation (under excitation) and its analysis, *Trans. Inst. Elect. Eng. Japan*, 101, 1981, pp. 347-354.
[7] T. Kataoka, T. Ishikawa, T. Takahashi, Analysis of a Hysteresis Motor with Over-excitation, *IEEE Trans. on Magnetics*, 18(6), 1982, pp. 1731-1733.
[8] T. Ishikawa, T. Kataoka, V curve of hysteresis motor, *IEE Proceedings-B, Electric Power Applications, Electric Power Applications*, 138(3), 1991, pp. 137-141.
[9] G. Wakui, I. Ohahi, K. Kurihara, Automatic Operation of Hysteresis Motor with Short Duration Over-excitation, *Electrical Engineering in Japan*, 103(6), 1983, pp. 98-105.
[10] T. Kubota, K. Kurihara, T. Tamura, Characteristics of PWM inverter-driven hysteresis motor with short-duration over-excitation, *International Conference on Electrical Machines and Systems (ICEMS)*, 2010, pp. 1429-1433.
[11] T. Kubota, T. Tamura, K. Kurihara, New Scheme for High-Efficiency Operation of PWM Inverter-Driven Hysteresis Motor with Short-Duration Over-excitation, *XIX International Conference on Electrical Machines (ICEM)*, 2010, pp. 1-6.
[12] T. Kubota, T. Tamura, K. Kurihara, High-Efficiency operation of PWM inverter-driven hysteresis motor with short-duration over-excitation, *International Conference on Electrical Machines and Systems, (ICEMS 2009)*, 2009, pp. 1-4.
[13] A. Halvaei Niasar, A. Ghanbari, Evaluation of Various Dynamic Modeling Methods of a Circumferential-Flux Hysteresis Motors, *in Proceedings of the 7th IEEE Power Electronics, Drive Systems & Technologies Conference (PEDSTC)*, 2016.
[14] A. Halvaei Niasar, A. Ghanbari, A. PirZadeh, An Improved Analytical Dynamic Modeling of Hysteresis Motor, *in Proceedings of the 24th Iranian Conference on Electrical Engineering (ICEE), May 10-12*, 2016.
[15] M.A. Rahman, Analytical Models for Poly phase Hysteresis Motor, *IEEE Trans. on Power Apparatus and Systems*, 92(1), 1973, pp. 237-242.
[16] IEEE standard for test procedures for magnetic cores, IEEE Std. 393-1991, *American National Standard (ANSI)* (1991).
[17] R.D. Jackson, M.A. Rahman, G.R. Slemon, Analysis and Determination of Ring Flux Distribution in Hysteresis Motors, *IEEE Trans. on Power Apparatus and Systems*, 102(8), 1983, pp. 2743-2749.
[18] A. Halvaei Niasar, A Novel Time Varying Dynamic Modeling for Hysteresis Motor, *Journal of Scientia Iranica, Sharif University of Technology*, 2016, (in Press).
[19] M.A. Rahman, A.M. Osheiba, Dynamic Performance Prediction of Poly Phase Hysteresis Motors, *IEEE Trans. on Industry Applications*, 26(6), 1990, pp. 1026-1033.
[20] C.M. Ong, *Dynamic Simulations of Electric Machinery*, Prentice-Hall Inc., 1998.
[21] E.V.C Sekhara Rao, P.V.N Prasad, orque Analysis of Permanent Magnet Hybrid Stepper Motor using Finite Element Method for Different Design Topologies, *International Journal of Power Electronics and Drive System (IJPEDS)*, 2(1), 2012, pp.. 107-116.
[22] Li Qian-Yu, Zhang Rui-Ping, Xiong Jian, The Research on Control Method of Variable Speed System of Permanent Magnet Synchronous Motor, *International Journal of Power Electronics and Drive System (IJPEDS)*, 12(9), 2014, pp. 6431-6436.

BIOGRAPHIES OF AUTHORS

S. H. Edjtahed received his B.Sc. degree from Tehran University in control engineering. In 2004 he received his M.Sc. degree form Amirkabir University (Tehran Polytechnic) in control engineering. Now he is a lecturer Department of Electrical and Computer Engineering, University of Kashan.

AmirHossein PirZadeh was born in Kashan, Iran in 1992. He received his B.Sc. and M.Sc. in 2014 and 2016 from University of Kashan, Kashan, Iran, in electrical engineering. His research interests include power electronics, analysis and control of electrical machines.

Abolfazl Halvaei Niasar was born in Kashan, Iran in 1974. He received his B.Sc., M.Sc., and Ph.D. in 1998, 2000, and 2008 from Isfahan University of Technology (IUT), University of Tehran (UT) and Iran University of Science and Technology (IUST) all in electrical engineering respectively. He is currently with the Department of Electrical and Computer Engineering, at University of Kashan, Kashan, Iran. His research interests are mainly PM and Brushless DC motor drives, sensorless drives, design and analysis of Electrical machines, DSP based control systems and industrial control systems engineering. Dr. Halvaei is a senior member of the Institute of Electrical and Electronics Engineers (IEEE).